

Evaluation of lateral ground deformation using sliding block model

Mohammad H. Baziar
University of Tehran, Iran

Ricardo Dobry
Rensselaer Polytechnic Institute, Troy, N.Y., USA

Mahmoud Alemi
Power Engineering Consultants (Moshanir), Tehran, Iran

ABSTRACT: A study is presented on the evaluation of lateral displacement at the Wildlife site in California, U.S.A., during the 1987 Superstition Hills earthquake. Newmark's rigid sliding block model is used as main analytical technique. A laboratory based approach, previously developed by the authors, is used to obtain the post-liquefaction steady-state shear strength of a very loose, recently deposited, layered fluvial silty sand susceptible to lateral spreading. The laboratory approach suggests a ratio of $S_u/\bar{\sigma}_v = 0.145$. The sliding block model, in conjunction with the yield acceleration obtained from this ratio and the available Wildlife site accelerogram, is successfully applied to predict the measured displacement. A parametric study is also included showing the effects of sliding block angle and groundwater elevation on the lateral displacement.

1 INTRODUCTION

Ground deformation due to liquefaction-induced lateral spreading of loose, saturated sand deposits constitutes one of the most common and destructive phenomena caused by earthquakes. A lateral spread typically involves predominately horizontal displacements of a large, superficial soil block, with the displacements, due to combined effect of static and seismic forces. Lateral spreads generally develop downhill on very mildly sloping terrain containing Late Holocene, loose, fluviually sedimented sand or silty sand. Permanent displacement ranging between a few centimeters and several meters have been observed in the U.S., Japan and other countries, causing damage to roads, canals, embankments, buried pipes and building foundations, Youd and Perkins (1987).

Clearly, the evaluation of engineering effects of liquefaction at a site for a given earthquake implies the ability of predicting the magnitude and spatial distribution of the permanent ground displacements. However, although we can currently predict if a site will liquefy or not with a reasonable degree of confidence using penetration charts, no such general method exists for the evaluation of the displacement. Intensive research efforts on the subject are currently underway especially in the United States and Japan (US-Japan, 1990). The magnitude of the displacements depends on the intensity and the duration of the ground shaking. Under the assumption that displacements accumulate

only during shaking, the use of Newmark's method (Newmark, 1965) in conjunction with the post-liquefaction steady-state or residual soil shear strength has been proposed.

2 WILDLIFE SITE

2.1 Location and characteristics

The Wildlife site is located near the Alamo River in the northern part of the Imperial Valley, California, U.S.A. Interest in this site started after it liquefied in 1981 during the Westmorland earthquake ($M_w = 5.9$), when it became clear that there were good chances of its experiencing other earthquakes and liquefying again in a few years. In 1982, the U.S. Geological Survey decided to instrument the site (Bennett, et al., 1984). In addition, a number of in-situ and laboratory investigations were conducted by several organizations, to document the characteristics of the site and to provide the data needed for the analysis of any future event. A summary of these measurements is given by Baziar (1991).

Three soil layers between the ground surface and buried accelerometer SM1 are discussed in this section. As described by Bennett, et al. (1984) and summarized in Fig 1, the deposit between 0 and 2.5 m consists of very loose and very soft interbedded micaceous sandy silt, silt and clayey silt. This is a very soft stratum, with a static cone resistance $q_c = 6 \text{ Kg/cm}^2$ and with most values of the Standard Penetration

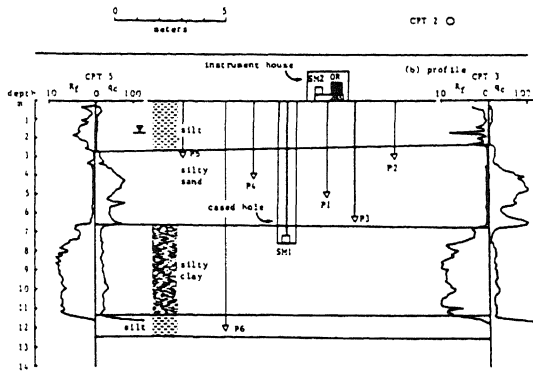


Figure 1. Cross-Section of Wildlife Site Showing Location of Piezometers (Bennett, et al., 1984)

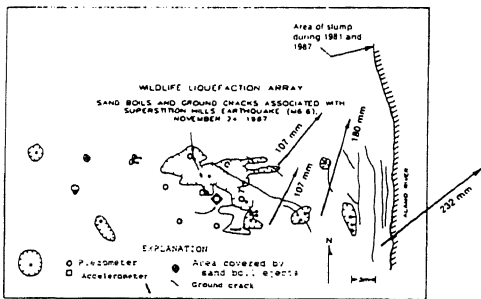


Figure 2. Sand Boils, lateral Spreading and Cracks at Wildlife Liquefaction Array (modified after, Holzer, et al., 1989b, Youd and Bartlett, 1988)

(SPT) Index (N) ranging from 1 to 3 blows/ft (Unit A).

The silty sand layer between 2.5 and 6.8 m containing the piezometers consists of two subunits. The upper unit between 2.5 to 3.5 m is a very loose to loose (N=5) moderately sorted sandy silt with small-scale cross bedding (Unit B₁). The lower subunit between 3.5 and 6.8 m is a loose to medium dense (N=6 to 13) well-sorted silty sand to very fine sand, with the coarsest sediment being at the bottom of the unit (Unit B₂).

The deposit below 6.8 m consists of medium to stiff clayey silt, and for all practical purposes it defines an impervious base for the liquefiable silty sand layer above it. Accelerometer SM1 is placed in this material at 7.5 m depth.

Figure 1 presents the cross section of the site with locations of the two strong motion accelerometer (SM2 at the ground surface and SM1 at the base of the liquefiable silty sand layer) and six piezometers (P1 to P6). The ground water level is at about 1.5 m depth, and the silty sand extends between 2.5 and 6.8 m; piezometers P1 to P5 are

located in the silty sand. Piezometer P6 is in a dense silt layer at about 12 m, separated from the liquefiable layer by a thick silty clay.

2.2 Lateral spreading in Wildlife

During the 1987 earthquake, the Wildlife site liquefied and developed lateral displacements toward the river ranging from 0 to 232 mm. Most significantly, for the first time, excess pore water pressure ratios of 100% were recorded in the field in a saturated sandy site during an earthquake (youd and Bartlett 1988, and Holzer, et al., 1989 a,b).

The 1987 records provided researchers with a unique opportunity of improving their understanding of the mechanics of seismic pore water pressure build-up, cracking and permanent displacement during lateral spreadings.

Figure 2 shows the value and direction of the recorded ground surface movements. The soil profile moved toward the river in generally North and East direction. As discussed by Dobry et al. (1992), the site had also shown revetment failure in the N15E direction during the 1981 Westmorland earthquake. It could be argued that the presence of this ground failure prior to 1987 probably controlled the movement of the site during the 1987 earthquake. An inclinometer casing extended to 8.8 m depth was also installed near the instrument array. This inclinometer recorded a 180 mm lateral displacement of the site toward the river in a N15E direction, with a maximum estimated shear strain of 4% concentrated in the upper part of the profile (Holzer, et al., 1989 a).

Figure 3 shows an idealized cross-section of the site in the N15E direction with more or less perpendicular to the long cracks in the zone of field instruments in Fig. 2. Dobry et al. (1989), using nonlinear one dimensional computer program, analyzed the pore pressure response of Wildlife site and found that the peak dynamic shear stresses on the top sublayer (2.5-3.5 m) are much higher than the estimated strength of this soil. Based on this, they suggested that the soil layers between the groundwater level and 3.5 m in depth are the most likely to have developed large strains and liquefied during the 1987 earthquake.

In other words, Dobry et al. (1989) suggested that yielding and lateral spreading associated with the liquefaction of loose layers A, B1 were responsible for this lateral movement. Holzer, et al. (1989a) based on post-earthquake monitoring of the inclinometer already mentioned, located near the cracks in Fig. 2, indicated that a large subsurface shear strain had

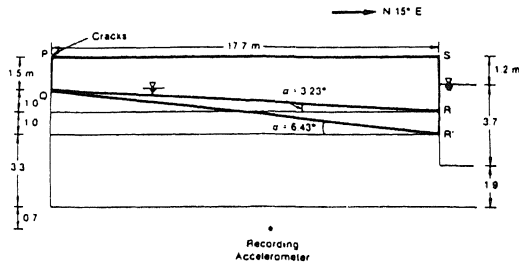


Figure 3. Soil Profile Assumed Failure Planes for Newmark Analyses, Wildlife Site, November 24, 1987 Earthquake (Baziar and Dorby, 1991)

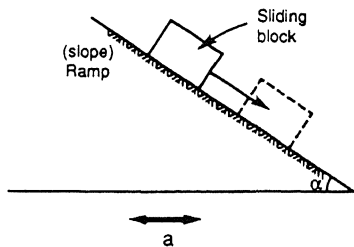


Figure 4. Sliding Block on the Top of the Ramp (Slope)

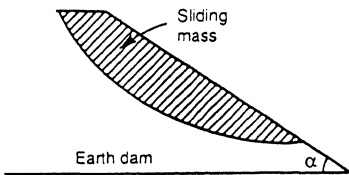


Figure 5. Sliding Block Model Used by Newmark

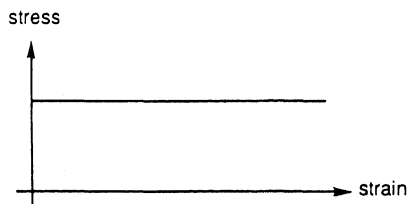


Figure 6. Rigid-Plastic System

occured in sublayer B1.

Based on the above information, the two failure mechanisms sketched in Fig. 3 were selected for rigid sliding block analyses. Both failure planes QR and QR' start at point Q defined by the intersection of the crack and the ground water level, and they end at the free face at the base of layers A and B1, respectively. These failure planes

define angles $\alpha=3.23^\circ$ and $\alpha=6.43^\circ$, used in the sliding block analyses to evaluate the lateral movement toward the river of rigid block PQRS or PQR'S.

3 SLIDING BLOCK MODEL

3.1 General

Figure 4 sketches the sliding block model proposed by Newmark (1965) to estimate permanent displacement of slopes and embankments due to earthquake shaking. The basic assumption is that when the ramp (slope) is accelerated up slope, the rigid block on top tries to follow it. However, when the ramp acceleration exceeds a certain limit, the block fails to follow the motion and slides down. If the acceleration changes sign cyclically, as is the case during earthquakes, the block may climb up during the downslope part of the cycle; this will happen if the level of acceleration is high enough. However, even in this case the net displacement at the end of each acceleration cycle will tend to be downward.

The maximum acceleration (yield acceleration) which can be transmitted to the sliding block before sliding occurs, is controlled by the slope angle and by the interface friction force between block and ramp. Newmark (1965) suggested that in soil where a well defined failure surface can develop, the motion occurs along such a surface, which can be taken as that assumed in the usual static stability analysis of the slope or embankment (Fig. 5). He further assumed that there is no relative motion between the block and the plane until the shear force reaches the limiting frictional resistance, whereafter sliding occurs without change in the shear force (rigid-plastic system). This neglects the elastic displacement, which is reasonable if the sliding deformation is large. Assuming a rigid plastic behaviour (Fig. 6) for the block, he calculated the displacement of the block by double integration of the input acceleration during the time that the total force parallel to the ramp acting on the block, was larger than the force that could be transmitted by the interface-block-ramp. The total force is generated by both gravity and earthquake action and the interface force is proportional to the soil strength.

3.2 Yield acceleration

Many investigators have studied the slope acceleration limit, a_y , (yield acceleration) beyond which a down slope movement of the block occurs.

For a ground acceleration parallel to the slope, Lambe and Whitman (1969)

calculated the yield acceleration for downslope movement of the block as :

$$a_y/g = \cos\alpha \cdot \tan\phi - \sin\alpha \quad (1)$$

where ϕ is the friction angle of the material in the slope, α is the slope angle with respect to the horizontal, and g is acceleration due to gravity.

In Equation 1, the shear strength of the soil and the corresponding friction force affect the yield acceleration of the block through angle ϕ , and the geometry of the slope affects it through angle α . As a drained ϕ is assumed and no effect of pore pressure build up during earthquake loading is taken into account, Equation 1 is in principle valid for dry sand or other granular soil.

Baziar (1991) studied the yield acceleration of a mild saturated silty sand slope. He used a laboratory approach to obtain the undrained static shear strength of a very loose, recently deposited, layered fluvial silty sand. From the laboratory results he obtained a ratio of $S_u/\bar{\sigma}_{1c} = 0.145$ where S_u =undrained shear strength, $\bar{\sigma}_{1c}$ =effective vertical consolidation stress. In the tests he used a fine silty sand taken from Lower San Fernando Dam. Because of the special water sedimentation method he used in his sample preparation where the silty sand was deposited in layers (see also Baziar and Dobry 1990) he argued that the same ratio can be applied to the field for the in-situ post-liquefaction shear strength of the same soil when it has been water sedimented.

In other words, he suggested a ratio of $S_u/\bar{\sigma}_v = 0.145$ for a layered silty sand recently deposited where $\bar{\sigma}_v$ is initial effective overburden pressure. Using this ratio he obtained an expression for the yield acceleration for the downslope movements:

$$a_y/g = (\bar{\sigma}_v/\bar{\sigma}_v) (S_u/\bar{\sigma}_v - \sin\alpha) \quad (2)$$

4 ANALYSIS OF WILDLIFE PROFILE

Figure 7 includes the NS component of the accelerogram recorded in 1987 at 7.5 m depth, below the liquefied soil where the ordinates of the original record were multiplied by a factor 1.05. This was done to account for the amplification of the motion between 7.5 m depth and the base of the sliding block, at 2 or 3 m depth, based on the recorded ground surface accelerogram and the site response analyses performed by Dobry, et al. (1989).

For the saturated loose layered silty sand deposit, $S_u/\bar{\sigma}_v = 0.145$ is assumed, consistent with the laboratory results on silty sand discussed by Baziar

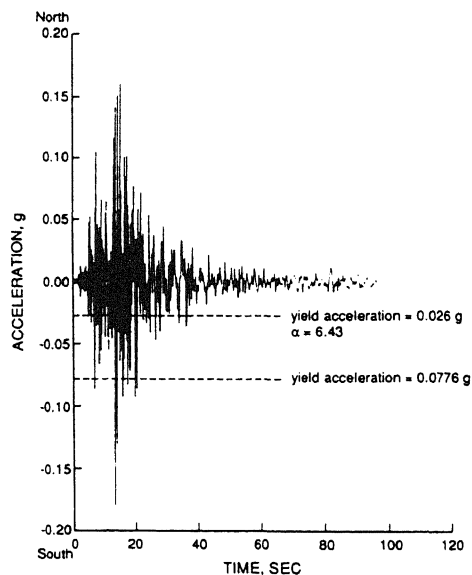


Figure 7. Input Acceleration Time History for Wildlife Site Analyses

(1991). Since the water table is assumed parallel to the ground surface and QR or QR' are also planes (Fig. 3), the representative $\bar{\sigma}_v, \bar{\sigma}_v$ and S_u for this failure mechanism can be taken at mid point of failure plane QR or QR'. Finally, with total unit weight $\gamma_t = 2$ grams/cm³ and buoyant unit weight $\gamma_b = 1$ gram/cm³ the corresponding yield acceleration for these two failure planes can be obtained.

The two values of the yield acceleration for downslope movements corresponding to the two soil blocks are superimposed on Fig. 7. These yield accelerations were obtained using Equation 2 and $S_u/\bar{\sigma}_v = 0.145$.

Figure 8 presents the displacement time histories calculated with the sliding block analyses for the two values of α and corresponding yield accelerations. In the analyses, the block was allowed only to slide downslope (toward the river), on the assumption that, in this case, material filling up the cracks did not permit a sliding back up of the block away from the free face. This assumption looks particularly reasonable for this case, in the light of relatively high uphill yield accelerations calculated assuming no restraint (0.176 and 0.21 g), for an earthquake record with a peak acceleration not exceeding 0.18 g.

For $\alpha=3.23^\circ$ (block PQRS), a total displacement of 1.9 cm is calculated at the end of the earthquake, while for $\alpha=6.43^\circ$ (block PQR'S), the calculated displacement is 31.7 cm. These two values bound the measured displacement of 18 cm, as illustrated by the figure, thus showing the

reasonableness of the assumed failure mechanism and value of $S_u/\bar{\sigma}_v$ used in the calculations. The relatively wide variation between these two calculated values also illustrates the sensitivity of the prediction to the selected value of the slope angle α .

Figure 9 draws a complete picture of the effect of the slope angle α on the calculated displacement. In this figure, a small displacement of less than 10 cm is calculated for slope angles up to 4° or 5° , with the displacement increasing rapidly for $\alpha > 5^\circ$. For $\alpha = 7^\circ$, the displacement is about 60 cm, for $\alpha = 6.43^\circ$ and 3.23° ($a_y = 0.0264$ and 0.0776 g), the displacements are 31.7 cm and 1.9 cm, respectively, corresponding to the values calculated in the previous section.

It is also interesting to evaluate the effect of the ground water table depth (Z_w) on the calculated lateral displacement. In all previous calculations, $Z_w = 1.5$ m was assumed. The calculations were repeated using the same input acceleration (Fig. 7) with Z_w ranging from 0 to 1.5 m for $\alpha = 6.43^\circ$. Figure 10 shows that as the water table becomes deeper, the value of the predicted displacement decreases. This is explained by the fact that as the water table depth increases, the ratio $\bar{\sigma}_v/\sigma_v$ in Equation 2 increases gradually from 0.8 toward 1.0 with the corresponding increase in yield acceleration a_y .

5 CONCLUSIONS

The concept of using a sliding block model for evaluation of ground displacement is briefly developed here. In this method, the main parameter to be obtained from the soil profile and properties or yield acceleration for the downslope displacements. The key question here is the determination of soil shear strength to use in the calculations. In this study a constant ratio between post-liquefaction shear strength (S_u) and effective pressure is used to calculate the yield acceleration of a very loose fluvial deposit of silty sand. Because of this assumption, the yield acceleration needed for a sliding block analysis of a lateral spread is a simple function of $S_u/\bar{\sigma}_v$, the ratio between total and effective vertical pressures, and the geometry of the sliding block.

Confirmation of the reasonableness of the approach is provided by the successful evaluation of the lateral displacement measured at the Wildlife site after the November 1987 earthquake as well as by the predicted influence of slope angle and depth of water table on the calculated displacements, made by Hamada et al. (1986).

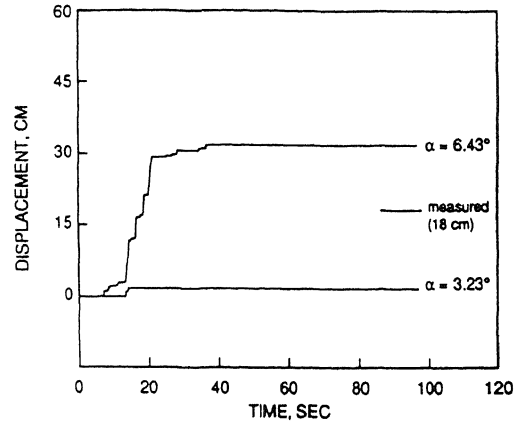


Figure 8. Measured and Predicted Displacement at Wildlife Site Using Newmark Analysis, November 24, 1987 Earthquake

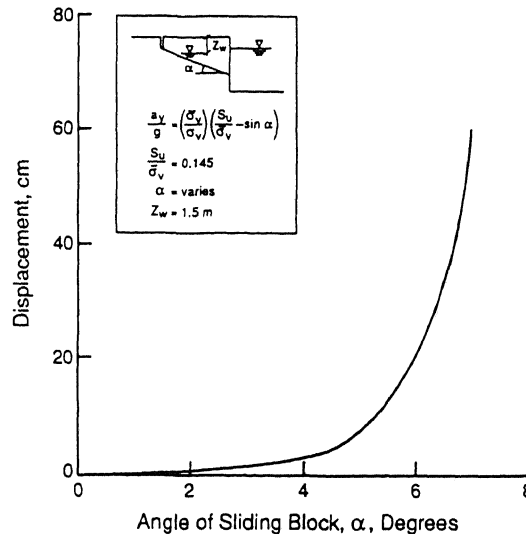


Figure 9. Effect of Sliding Block Angle of the Wildlife Site on Predicted Displacement

ACKNOWLEDGEMENT

This research was supported by the National Center for Earthquaks Engineering Research of U.S.A. Miss Sh. Tavakoly patiently helped to type this manuscript. This help and support is gratefully acknowledged.

REFERENCES

- Baziar, M.H. (1991) "Engineering Evaluation of permanent Ground Deformation due to Seismically-Induced Liquefaction," Ph.D. Thesis. Dept. of Civil Engineering, Rensselaer Polytechnic Institute, Troy, Ny 12180.

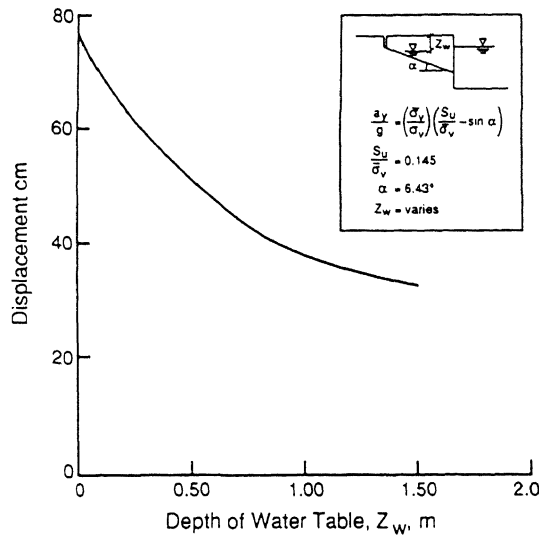


Figure 10. Effect of Depth of Water Table of Wildlife Site on Predicted Displacement

- Baziar, M.H., and Dobry, R. (1991) "Liquefaction Ground Deformation Predicted from Laboratory Tests," Proceedings, Second International Conference on Recent Advances in Geotechnical Earthquake Engineering and Soil Dynamics, St. Louis, MO, USA, March, Vol. I, pp. 451-458.
- Bennett, M.J., McLaughlin, P.V., Sarmiento, J.S., and Youd, T.L. (1984) "Geotechnical Investigation of Liquefaction Sites, Imperial Valley, California," Open-File Report 84-252, U.S. Geological Survey, Menlo Park, California.
- Dobry, R., Baziar, M.H., O'Rourke, T., Roth, B., and Youd, T.L., (1992) "Liquefaction and Ground Failure in the Imperial Valley, Southern California, During 1979, 1981, and 1987 Earthquakes," Case Studies of Earthquakes for Large Ground Deformation, O'Rourke, T. and Hamada, M. (eds.), in press.
- Dobry, R., Elgamal, A.W., Baziar, M.H., and Vucetic, M. (1989) "Pore Pressure and Acceleration Response of Wildlife Site During the 1987 Earthquake," Proceedings, Second U.S.-Japan Workshop on Liquefaction, Large Deformation and Effects on Buried Pipelines, Niagara Falls, New York, pp. 145-160.
- Hamada, M., Yasuda, S., Isoyama, R., and Emoto, K. (1986) "Study on Liquefaction Induced Permanent Ground Displacements." Report for the Association for the Development of Earthquake Prediction.
- Holzer, T.L., Youd, T.L., and Hanks, T.C. (1989a) "Dynamics of Liquefaction During the 1987 Superstition Hills, California Earthquake," Science, Vol. 244, pp. 56-59.
- Holzer, T.L., Youd, T.L., and Bennett, M.J. (1989b) "In-Situ Measurement of Pore Pressure Build Up During Liquefaction," Proceedings, 20th Joint Meeting of the U.S.-Japan Cooperative Program in the Natural Resources, panel on Wind and Seismic Effects, U.S. Department of Commerce.
- Lambe, T. William, and Whitman, Robert V. (1969) Soil Mechanics, John Wiley & Sons, Inc., New York.
- Newmark, N.M. (1965) "Effect of Earthquakes on Dams and Embankments," Geotechnique, Vol. 5, No. 2.
- U.S.-Japan, (1990) Proceedings, Third Workshop on Liquefaction Ground Deformation and Their Effects on Lifeline Facilities, Hamada, M., and O'Rourke, T. D., editors, San Francisco, December 17-19.
- Youd, T. L., and Perkins, D. M., (1987) "Mapping of Liquefaction Severity Index," JGED, ASCE, Vol. 113, No.11, November, pp. 1374-1392.
- Youd, T.L., and Barlett, S.F. (1988) "U.S. Case Histories of liquefaction-Induced Ground Failure," Proceedings, First Japan-U.S. Workshop on Liquefaction, Large Ground Deformation, and Their Effects on Lifeline Facilities, Tokyo, Japan, pp. 22-31.